



Electrical properties of Poly(ethylene glycol dimethacrylate-*n*-vinyl imidazole)/Single Walled Carbon Nanotubes/*n*-Si Schottky diodes formed by surface polymerization of Single Walled Carbon Nanotubes

Muhitdin Ahmetoglu (Afrailov)^a, Ali Kara^{b,*}, Nalan Tekin^c, Saadet Beyaz^c, Hakan Köçkar^d

^a Department of Physics, Uludağ University, 16059, Görükle, Bursa, Turkey

^b Department of Chemistry, Uludağ University, 16059, Görükle, Bursa, Turkey

^c Department of Chemistry, Kocaeli University, 41380, Umuttepe, Kocaeli, Turkey

^d Department of Physics, Balıkesir University, 10145, Çağış, Balıkesir, Turkey

ARTICLE INFO

Article history:

Received 12 January 2011

Received in revised form 18 August 2011

Accepted 18 August 2011

Available online 24 August 2011

Keywords:

Metal semiconductor-structure

Schottky barrier

Single Walled Carbon Nanotube

n-vinyl imidazole

ABSTRACT

In this paper we report the electrical characteristics of the Schottky diodes formed by surface polymerization of the Poly(ethylene glycol dimethacrylate-*n*-vinyl imidazole)/Single Walled Carbon Nanotubes on *n*-Si. The Single Walled Carbon Nanotubes were synthesized by CVD method. The main electrical properties of the Poly(ethylene glycol dimethacrylate-*n*-vinyl imidazole)/Single Walled Carbon Nanotubes/*n*-Si have been investigated through the barrier heights, the ideality factors and the impurity density distribution, by using current–voltage and reverse bias capacitance voltage characteristics. Electrical measurements were carried out at room temperature. Poly(ethylene glycol dimethacrylate-*n*-vinyl imidazole)/Single Walled Carbon Nanotubes/*n*-Si Schottky diode current–voltage characteristics display low reverse-bias leakage currents and average barrier heights of 0.61 ± 0.02 eV and 0.72 ± 0.02 eV obtained from both current–voltage and capacitance–voltage measurements at room temperature, respectively.

© 2011 Elsevier B.V. All rights reserved.

1. Introduction

Interfaces between thin metal layers and semiconductors are used in optical detectors, solar cells [1] and chemical sensors [2,3]. The transport properties of such Schottky diodes and the dependence of the transport parameters on preparation are of essential importance for the device performance. Metal–semiconductor interfaces may be characterized by photoelectrical and current–voltage measurements [4,5].

The metallization of semiconductor surfaces is still mostly performed in vacuum by evaporation or sputtering. The process, itself, is of great technological importance for preparing Schottky barriers and ohmic contacts in electronic devices.

Carbon nanotubes possess chemical and mechanical properties that exceed those of many other materials. They are considered as innovative materials and have been most intensely studied in the chemistry, condensed matter physics and material science domains. The unique electronic and mechanical properties of Single Walled Carbon Nanotubes (SWCNT) have made them suitable for several applications in nanoelectronics and quantum computing, as gas sensors, fillers in polymer, ceramic and metal composites [6] and even hydrogen storage [7,8]. Studies have shown that SWCNT can be used as field effect transistors [9] and they are excellent candidates for low-resistance interconnects [10,11].

The combination of the very low densities with mechanical and other physical properties of the carbon nanotubes makes them ideal candidates for high performance polymer composites. They may represent the next generation of carbon fibers if high quality (high crystallinity) nanotubes are available in large quantities and the dispersion problem of these nanoscale materials in the polymer is solved. Several methods such as arc-discharge, laser ablation, and catalytic chemical vapor deposition (CCVD) have been effectively used for SWCNT synthesis. It is generally accepted that CCVD is a promising method for producing SWCNT with high purity on large scale [12]. One challenge in the fabrication of carbon nanotube-reinforced composites is the homogeneous dispersion of the carbon nanotubes in the polymer matrix and its relation to the uniformity of properties.

In the present paper we report of an experimental study of the current–voltage ($I-V$) and capacitance–voltage ($C-V$) measurement results of Schottky diodes formed by surface polymerization of carbon nanotube.

2. Experimental procedure

2.1. Materials

Ethylene glycol dimethacrylate (EGDMA) was obtained from Merck (Darmstadt, Germany), purified by passing through active alumina and stored at 4 °C until use. *N*-Vinyl imidazole (VIM) from Aldrich

* Corresponding author. Tel.: +90 2242941733; fax: +90 2242941899.
E-mail address: akara@uludag.edu.tr (A. Kara).

(Steinheim, Germany) was distilled under vacuum (74–76 °C, 10 mm Hg). 2,2-Azobisisobutyronitrile (AIBN) was obtained from Fluka A.G. (Buchs, Switzerland). All other chemicals were of reagent grade and were purchased from Merck AG (Darmstadt, Germany). C₂H₂, H₂, N₂ and He gasses with high purity were obtained from Yalız Society (Gebze-Turkey). MgO from Sigma and Ni(NO₃)₂·6H₂O from (Karlsruhe, Germany) were used as catalyst support and catalyst respectively.

2.2. Preparation of single walled carbon nanotubes

The SWCNTs were synthesized by CVD method. Prior to the synthesis, the support containing the catalyst was prepared. The catalyst loading took place by impregnation of MgO (Sigma) in an aqueous 1% Ni (NO₃)₂·6H₂O solution for 24 h and leave it to dry in an oven at 303 K. The dried support was further purged with He at room temperature in the tubular furnace. The deposited nickel (II) ions were reduced to metallic nickel nanoparticles under a He/H₂ flow of 60 ml/min (H₂ 99.998%), at 853 K for 3 h. Then the furnace temperature was increased at a rate of 10 °C/min up to 973 K and CVD took place for 20 min by replacing H₂ with C₂H₂ (20 ml/min C₂H₂:99.8, 300 ml/min He). The temperature was increased at a rate of 10 °C/min and CVD took place isothermally at 973 K for 3 h under C₂H₂/He flow (10 ml/min C₂H₂ 99.6%, 600 ml/min He 99.999%). Then the temperature of the tubular furnace was decreased to room temperature under the flow.

One-sided polished n-Si (111) samples, phosphorus-doped, 1–20 Ω cm were used as substrate. They were cleaned following cleaning procedure [13], which means degreasing in 2-propanol under reflux for 2 h and then boiling alternating for 15 min in basic and acidic H₂O₂ solutions. Prior to each experiment the substrates were etched for 1 min in 20% HF (Merck, VLSI Selectipur) to remove the oxide layer. Ohmic contacts were formed by vacuum evaporation of an Au layer on the back of the wafers after the etching procedure.

2.3. Preparation of Poly(ethylene glycol dimethacrylate-*n*-vinyl imidazole)/Single Walled Carbon Nanotubes/*n*-Si films

The feed composition menu for the preparation of the Poly(ethylene glycol dimethacrylate-*n*-vinyl imidazole)/Single Walled Carbon Nanotubes [P(EV)-SWCNT]/*n*-Si is shown in Table 1. About 1.5 mL of each solution, consisting of toluene, EGDMA, VIM, AIBN, and SWCNT, were used to prepare the [P(EV)-SWCNT]/*n*-Si films. The mixture was degassed 30 min by nitrogen purging prior to the addition of the initiator, AIBN. Then the polymerization was conducted for 2 h at 25 °C under stirring and nitrogen atmosphere. After the 2 h, the solution was transferred into a known area (1 cm²) – surface of *n*-type Si and the polymerization was continued for 24 h at 70 °C in an oven. The thickness of the films was 300 μm.

One-sided polished n-Si (111) samples, phosphorus-doped, 1–20 Ω cm plates were used as substrate. They were cleaned following the cleaning procedure in ref.[13], i.e. degreasing in 2-propanol under reflux for 2 h and then boiling alternatively several times for 15 min in basic and acidic H₂O₂ solutions. Prior to each experiment the substrates were etched for 1 min in 20% HF (Merck, VLSI Selectipur) to remove the oxide layer. Ohmic contact was formed by vacuum evaporation of a Au layer on the back of the n-Si after the standard etching procedure. P(EV)-SWCNT was polymerize on n-Si

semiconductor, a surface of 1% Sb doped Au, made ohmic contact. Top ohmic contacts on the P(EV)-SWCNT were formed by silver contact paste.

Textural analysis of the [P(EV)-SWCNT]/*n*-Si films was characterized using a Carl Zeiss Evo 40 (Germany) SEM and operation voltage is 10 kV. The *I*–*V* measurements were performed using a Keithley (Keithley Instruments Ohio, USA) 6517A electrometer and *C*–*V* measurements were carried out at room temperature with a Keithley 590/1M *C*–*V* Analyzer. All measurements were controlled by a computer via an IEEE – 488 standard interfaces so that the data collecting, processing and plotting could be accomplished automatically.

3. Results and discussion

The surface morphology of the SWCNT was observed by scanning electron microscopy (SEM) as shown in Fig. 1. Fig. 1a shows a SEM image of the SWCNT prepared after the polymerization. From Fig. 1b, it can be seen that the SWCNT were fully covered by the polymer. The electrical characterizations of the device were achieved through *I*–*V* and *C*–*V* measurements at 300 K. The results of the formation of a Schottky barrier between the [P(EV)-SWCNT]/*n*-Si layer and *n*-doped Si (111) at room temperature in shown in Fig. 2. The reverse and forward currents of the diodes demonstrate the rectifying properties; the rectification coefficient was 112.58, defined as ratio of the forward current and reverse current at the same voltage. The current through

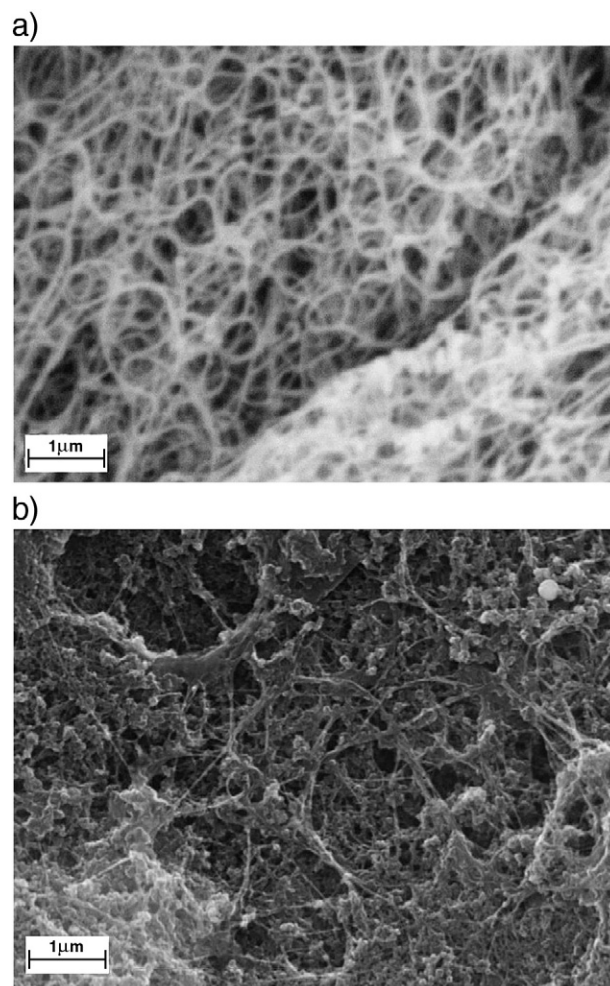


Fig. 1. SEM images of (a) SWCNTs and (b) SWCNTs embedded in P(EV).

Table 1
Feed composition used for the polymerization.

EGDMA	VIM	AIBN	Toluene	SWCNT
0.3 mL	0.5 ml	0.050 g	1.5 mL	0.020 g

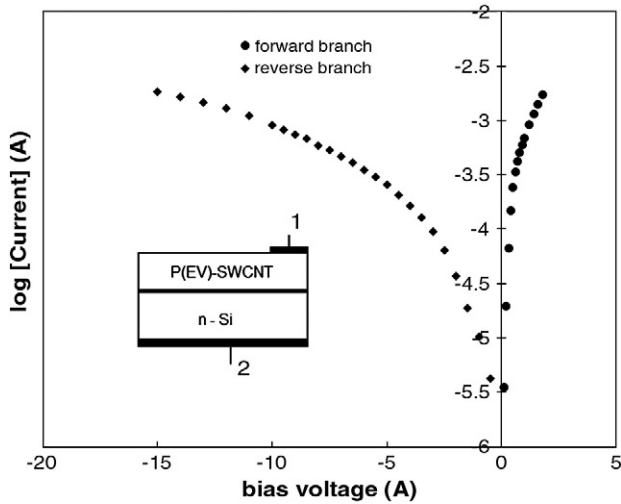


Fig. 2. The experimental forward and reverse bias current versus voltage characteristics in a linear scale of $[P(EV)\text{-}SWCNT]/n\text{-Si}$ Schottky barrier diodes at room temperature. In the inset showing the cross section of diode structure: 1, 2 – ohmic contacts.

a Schottky barrier diode at a forward bias V , based on the thermionic emission theory, is given by the relation [14],

$$I = I_0 \exp\left(\frac{qV}{nKT}\right) \left[1 - \exp\left(-\frac{qV}{KT}\right)\right] \quad (1)$$

where I_0 , the saturation current density, is given by

$$I_0 = A^*AT^2 \exp\left(-\frac{q\phi_{b0}}{kT}\right) \quad (2)$$

where q is the electron charge, V is the forward bias voltage, k is the Boltzmann constant, T is the absolute temperature, A , is the effective diode area ($A = 2.25 \text{ mm}^2$), $A^* = 4\pi qm^*k^2/h^3$ is the effective Richardson constant of $110 \text{ A/cm}^2 \text{ K}^2$ for n -type Si, ϕ_{b0} is the zero bias apparent barrier height (BH) and n is the ideality factor. The saturation current density I_0 was derived by extrapolation of the linear forward part to the current axis which was found to be $7.6 \times 10^{-5} \text{ A}$ (see Fig. 2), in agreement with the reverse bias current. The ideality factor is calculated from slope of the linear region of the forward bias $\ln I - V$ (in semi-log scale) plot and can be written from Eq. (1) as (see Fig. 3):

$$n = \frac{q}{kT} \left(\frac{dV}{d(\ln I)} \right) \quad (3)$$

The zero-bias barrier height ϕ_{b0} is given by:

$$\phi_{b0} = \frac{kT}{q} \ln\left(\frac{A^*AT^2}{I_0}\right) \quad (4)$$

The semilog-forward bias $I - V$ characteristics of the $\text{Cu}/n\text{-Si}(111)$ Schottky barrier diodes at room temperature are shown in Fig. 3. The experimental values of ϕ_{b0} and n , were determined from intercepts and slopes of the forward $\ln I$ versus V plot, respectively. The experimental values of 2.4 and 0.61 ± 0.02 eV were obtained for the ideality factor (n) and zero bias barrier height (ϕ_{b0}), respectively.

The bias dependence of the reverse current, often referred to as the soft reverse characteristic, cannot be explained within thermionic emission theory across a sharp barrier using Eq. (1). It may be due to the inhomogeneous Schottky barrier which softens the reverse characteristics significantly [15]. Additionally, tunneling contacts, parallel to the Schottky diode, may be formed on thin oxide layers around the etched window during evaporation.

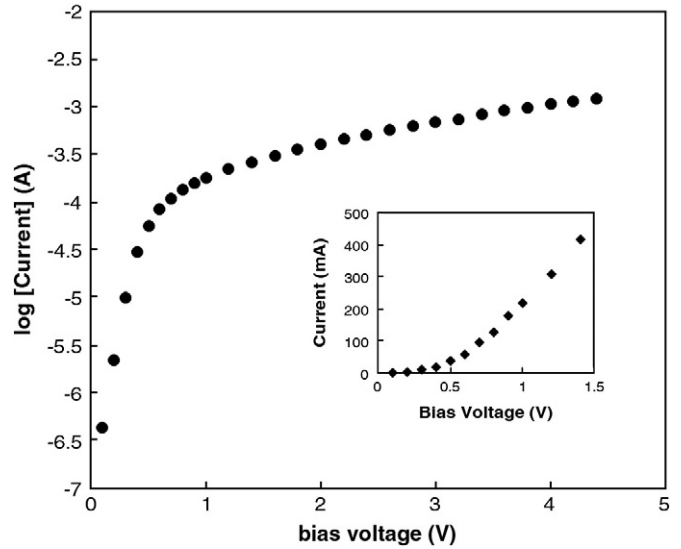


Fig. 3. The semilog and linear (in the inset) forward bias $I - V$ characteristics of $[P(EV)\text{-}SWCNT]/n\text{-Si}$ Schottky barrier diodes at room temperature.

The $C - V$ characteristics are one of the fundamental properties of the Schottky barrier diodes structure. Fig. 4 shows the capacitance-voltage characteristics taken at a temperature $T = 300 \text{ K}$ and frequency $f = 1 \text{ MHz}$. The characteristics are satisfactorily described by the dependence $C^{-2} \sim f(V)$, typical of an abrupt junction. The $C - V$ dependence can be interpreted by the law,

$$\frac{1}{C^2} = \frac{2(V_R + V_B)}{q\epsilon_s N_D A^2} \quad (5)$$

Where A is the area of the diode, V_R the reverse bias voltage, V_B is the built in (diffusion) potential at zero bias and is determined from the extrapolation of the $1/C^2 - V$ plot to the V -axis, ϵ_s is the dielectric constant of the Si, q is the electronic charge and N_D is the doping concentration.

The gradient of the $C^{-2} = f(V)$ curve leads to a carrier concentration in the Si $N_d = 9.87 \times 10^{15} \text{ cm}^{-3}$. The intercept of C^{-2} with the voltage axis give us the value of zero bias barrier height ϕ_{C-V} which was found to be $0.72 \pm 0.02 \text{ V}$. The ϕ_{C-V} are slightly larger than the ϕ_{I-V} (zero bias barrier height obtained from $I - V$ measurements, see inset of

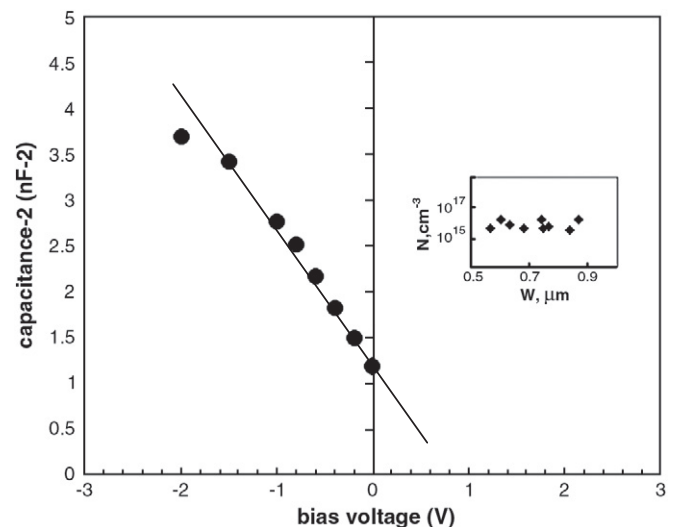


Fig. 4. The room temperature reverse bias $1/C^2 - V$ characteristics of $[P(EV)\text{-}SWCNT]/n\text{-Si}$ Schottky barrier diodes. In the inset the calculated doping profile.

Fig. 3) this difference is explained due to an interface layer or to trap states in the substrate, the effect of the image force and barrier in homogeneities [16].

The non-uniformity of doping at the interface should manifest itself when considering the impurity density distribution; $N(x)$ is directly proportional to the first derivative of $1/C^2$ with respect to V and is given by [17],

$$N(x) = \frac{2}{q\epsilon_s} \left[-d \left(\frac{1}{C^2} \right) \right]^{-1}. \quad (6)$$

The above equation and relation $C = \frac{\epsilon_s A}{W}$ were used to compute the doping profile in the inset of Fig. 4 (the majority carrier densities versus depth (W) across the depleted zone). It is seen that, the impurity density distribution is very uniform with average doping concentration of $N_d = 9.8 \times 10^{15} \text{ cm}^{-3}$. No information was obtained at the interface ($x = 0$), as is typical for doping profiles obtained from $C - V$ measurements. This is because the capacitance measurement was limited to small forward bias voltages since the forward bias current and the diffusion capacitance affect the accuracy of the capacitance measurement.

4. Conclusions

In this work we investigated the main electrical properties of the Schottky diodes formed by surface polymerization of the $[P(EV)\text{-}SWCNT]/n\text{-Si}$, through the barrier heights, the ideality factors and the impurity density distribution, by using current–voltage and reverse bias capacitance voltage characteristics. $P(EV)$ provided to create a

good contact of the $SWCNT$ on the n -type Si . Electrical measurements were carried out at room temperature. The distribution density of carriers throughout $[P(EV)\text{-}SWCNT]/n\text{-Si}$ Schottky barrier structures, derived from $C - V$ data, was used to calculate the majority carrier densities versus depth (W) across the depleted region and the impurity density distribution is very uniform with average doping concentration of $N_d = 9.8 \times 10^{15} \text{ cm}^{-3}$.

References

- [1] S.M. Sze, Physics of Semiconductor Devices, 2nd ed., Wiley, New York, 1981.
- [2] H. Nienhaus, H.S. Bergh, B. Gergen, A. Majumdar, W.H. Weinberg, E.W. McFarland, Phys. Rev. Lett. 82 (1999) 446.
- [3] X.J. Huang, Y.K. Choi, Sens. Actuators B-Chem. 122 (2007) 659.
- [4] A.I. Prokopyev, S.A. Mesheryakov, Measurement 33 (2003) 135.
- [5] M. Prietsch, Phys. Rep. 253 (1995) 163.
- [6] N. Grobert, Mater. Today 10 (2007) 28.
- [7] S.B. Kayiran, F.D. Lamari, B. Weinberger, P. Gabelle, L. Firlej, P. Bernier, Int. J. Hydrogen Energy 34 (2009) 1965.
- [8] S.B. Kayiran, F.D. Lamari, D. Levesque, J. Phys. Chem. B 108 (2004) 15211.
- [9] P. Avouris, J. Chen, Mater. Today 9 (2006) 46.
- [10] H. Wolfgang, G.S. Duesberg, A.P. Graham, F. Kreupl, M. Liebau, W. Pamler, R. Seidel, E. Unger, Microelectron. Eng. 83 (2006) 619.
- [11] F. Kreupl, A.P. Graham, G.S. Duesberg, W. Steinhögl, M. Liebau, E. Unger, W. Hönlein, Microelectron. Eng. 64 (2002) 399.
- [12] S.-M. Tan, S.-P. Chai, W.-W. Liu, A.R. Mohamed, J. Alloy Comp. 477 (2009) 785.
- [13] M.L. Minford, F. Maroun, R. Cortes, P. Allonque, A.A. Pasa, Surf. Sci. 537 (2003) 95.
- [14] E.H. Rhoderick, R.H. Williams, Metal-Semiconductor Contacts, Clarendon Press, Oxford, 1988.
- [15] J.P. Sullivan, R.T. Tung, M.R. Pinto, W.R. Graham, J. Appl. Phys. 70 (1991) 7403.
- [16] M. Said, A. Keffous, S. Mama, Y. Belkacem, H. Menari, Appl. Surf. Sci. 236 (2004) 66.
- [17] A. Sellai, M.S. Raven, M. Henini, Eur. Phys. J. 9 (2000) 131.